CrossMark

Effect of Size, Content and Shape of Reinforcements on the Behavior of Metal Matrix Composites (MMCs) Under Tension

A. Paknia, A. Pramanik, A.R. Dixit, and S. Chattopadhyaya

The objective of this research was to investigate the mechanical behavior of metal matrix composites (MMCs) 6061 aluminum, reinforced with silicon carbide particles, under unidirectional tensile loading by finite element analysis. The effects of particle's shape, size and content on the tensile properties of the composites were studied and compared with each other. In addition, stress and strain distributions and possible particle fracture or debonding were investigated. It was found that, among different shapes, a certain shape of reinforcement particle provided better tensile properties for MMCs and, within each shape category, composites with smaller particle size and higher particle content (20%) also showed better properties. It was also found that when the reinforcement content was 10%, the effects of shape and size of the particles were negligible. Not only interfacial length between the reinforcement and matrix materials, but also state of matrix material, due to the presence of the reinforcement particles, affected the stiffness of the MMCs. In almost all of the cases, except for MMCs with triangular particles, when the stress increased, with the increase in the applied positive displacement, the stress distributions remained unchanged.

1. Introduction

MMCs particularly aluminum-based particle-/fiber-reinforced composites have a high strength-to-weight ratio and wear resistance. Ceramic fiber-/particulate-/whisker-reinforced metal matrix composites (MMCs) have had increased applications due to their improved mechanical properties (e.g., improved strength, stiffness and wear resistance) over unreinforced alloys. The demand of new industrial applications for high performance composite materials has driven research efforts in the field of materials engineering (Ref 1). For example, the low wear resistance of aluminum alloy can be overcome by addition of ceramic particles, such as SiC or Al_2O_3. Aluminum alloy-based MMC is desirable because of its lower density, increased toughness and corrosion resistance in harsh environmental conditions (Ref 2).

Mechanical properties of MMCs have been studied for several decades by using numerical methods as well as experimental analyses for prediction of the overall properties of composites. Prabu et al. (Ref 3) developed a 2D microstructure-based FEA models to study the mechanical behavior of MMC. Their model took into account the randomness and clustering effects or the particle arrangement on stress–strain response and the failure behaviors. Huang et al. (Ref 1) used

FEA to evaluate the elastic and plastic properties of aluminum/alumina composite materials with ultrafine microstructure, and the matrix material was found to be an important factor influencing the mechanical properties of the composites.

Yan et al. (Ref 4) used finite element method to investigate the effect of particle size on the deformation behavior of the MMCs. Their results indicated that, at a constant particle volume fraction, there was a close relationship between the particle size and the deformation behavior of the composites. Several studies investigated the effect of reinforcement particle size on the mechanical properties of $Al-SiC_p$ composites. Varma et al. (Ref 5) explored low strain yielding behavior of SiC_p-reinforced Al-Cu-Mg alloy matrix composites with varying reinforcement sizes, such as 1.4, 15.8 and 62.8 μm under controlled strain deformation of 1.5% in both tension and compression. The actual yielding in all the MMCs occurred at lower stress levels in compression than in tension. These were attributed to the distribution of residual stresses in the matrix of MMCs generated due to the large difference in coefficient of thermal expansion between the matrix and the reinforcement.

Wang et al. (Ref 6) studied the effects of particle size and distribution on the mechanical properties of the SiC particle-reinforced Al-Cu alloy composites. It was shown that the small ratio between matrix/reinforcement particle sizes and increased mixing time provided more uniform distribution of the SiC particles in the matrix. This distribution resulted in higher yield strength, ultimate tensile strength and elongation. Yield strength and ultimate tensile strength of the composite increased with the decrease in particle size while the elongation decreased along with particle size. Ductile fracture of the matrix accompanied by the "pull-out" of the particles from the matrix occurred when reinforced particles were smaller. However, dominant fracture mechanism of the composites with larger particles was ductile fracture of the matrix, accompanied by the SiC particle fracture. Chawla et al. (Ref 7) studied SiC volume content and particle size on the fatigue behavior of 2080 Al

A. Paknia and A. Pramanik, Department of Mechanical Engineering, Curtin University, Bentley, WA, Australia; and A.R. Dixit and S. Chattopadhyaya, Department of Mechanical Engineering, Indian School of Mines, Dhanbad, Jharkhand 826004, India. Contact e-mail: alokesh.pramanik@curtin.edu.au.

alloy. They found that the increase in volume content and decrease in particle size resulted in an increase in fatigue resistance.

Hall et al. (Ref 8) studied the effects of particle's size, volume fraction and matrix strength on the stress-controlled axial fatigue behavior and the probability of particle fracture for 2124 aluminum alloy, reinforced with SiC particles. It was noted that the strength and fatigue life increased with the decrease in particle size and increase in volume fraction. The frequency of particle fracture during crack propagation was found to be dependent on matrix strength, particle size and volume fraction and maximum crack tip stress intensity. Although composites reinforced with smaller particles possessed better mechanical properties, larger reinforced particles gave better mechanical results in some cases. Ganesh and Chawla (Ref 9) investigated extrusion-induced particle orientation on the mechanical behaviors of metal matrix composites and noted that the composites demonstrated higher Young's modulus and tensile strength along the longitudinal direction (parallel to the extrusion axis) than that in the transverse direction. The range of anisotropy increased with the 20% volume content, due to the effect of the SiC reinforcement that increased the Young's modulus and tensile properties.

The above discussion clearly shows that there are huge researches on the effects of reinforcements on mechanical properties of MMCs, while some of these effects were consistent in different studies. However, inconsistencies about the effects of the reinforcement particle' size, on the behavior of the particle-reinforced MMCs, were experienced by O'Donnell et al. (Ref 10) and Narayanasamy et al. (Ref 11) which were due to the other dominant factors. In addition, the distribution of stress and strain under uniaxial tension was never investigated for different size, content and shape of reinforcements, though these are imperatively needed for a better design of MMCs. To address the above issues, this research modeled and investigated MMCs with four different reinforcement particle shapes and each shape with three different sizes and also three different reinforced contents. The stress distributions in MMCs and their vector directions in the vicinity of the reinforcement particles were also investigated. From these data, composites with different shapes, sizes and percentages of reinforcement particles were compared with each other, based on their mechanical properties. These results can assist manufacturers to have reliable data about the MMC's behaviors for any future improvements.

2. Finite Element Modeling

Total thirty-six study cases were considered in this investigation. For the ease of comparison between the results, the size of the MMC blocks remained constant. All the finite element models had a homogeneous distribution of reinforcement particles which gave the best results, exclusive of homogeneity variable that could sway the judgement about the particle's shape, size and content effects. The finite element software, ANSYS, was used to develop the models and generate the results. Composites with three different sizes of circular SiC particles, with 6, 12 and 24 μm in diameter, were modeled. Also, for each particle size three different contents of 10, 15 and 20% were considered. Total of nine study cases were

created for MMCs with circular particles. For other shapes, the area of the reinforcement particle remained constant (=area of the circular particle), and the lengths of the sides for equilateral triangle, square and rectangle shapes were calculated accordingly. Therefore, all four shapes had the same area but different perimeters. A constant positive displacement was applied on the blocks, and the tensile properties under this displacement were explored. As the block size and the displacement were constant, the macroscopic (overall) strain value in all of the cases remained constant. To induce a tensile force, the block was constrained, on the opposite side of the applied displacement, in Y-axis direction and also to avoid block's sideway movements, a middle node in the same side was constrained in X-axis direction (Fig. 1).

2.1 Number, Size and Shape of Particles in Each Case Study

The dimensions of the tensile blocks were selected as to have the number of particles, in each study case, an integer. This simplified having the exact required volume percentages of the reinforcement particles for the study cases. Based on values in Table 1, the area of the tensile block needed to be 27,159 μm^2, from which the block's dimensions were calculated as 329.5 μm long and 82.4 μm wide. The aspect ratio of 1:3 was selected for the rectangular reinforcement particles. This was based on a reasonable assumption to have a correct shape representation.

2.2 Material Properties

The MMC work material was a 6061 aluminum alloy, reinforced with silicon carbide particles. The reinforcement was considered as a linear isotropic material, following the generalized Hook's law. The material properties of the particles were: Young's modulus = 400 GPa and Poisson's ratio = 0.17. For the 6061 Al matrix, a temperature-independent multilinear kinematic hardening material model (available in ANSYS), and its associated flow rule, was used. The properties of the matrix were: Young's modulus = 71.6 GPa, yield strength = 125 MPa, shear modulus = 1.48 GPa and Poisson's ratio = 0.33 (Ref 12, 13). Figure 2 represents stress–strain curves included into the analysis for matrix and particles.

2.3 FEA Element Type and Behavior

This study used structural solid Plane 183 element for the two-dimensional analysis. To understand the effect of the reinforcement particles more easily, plane strain element behavior was selected in this study. Particles were assumed to be perfectly bonded to the matrix material. The number of steps in ANSYS was determined automatically, according to the convergence results of each model. Composites were modeled and meshed with manual sizing to achieve the best convergence and accuracy of the results. The meshed blocks of MMCs with circular reinforcement particles are shown in Fig. 3.
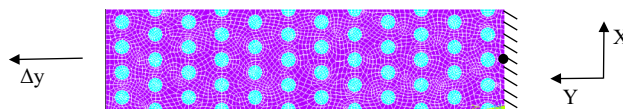

Fig. 1 Block's displacement and constraints

Table 1 Number and size of particles

Reinforcement content	Diameter of circle ⊙			Sides of equilateral triangle △		
	6 µm	12 µm	24 µm	8.08 µm	16.16 µm	32.32 µm
10%	96	24	6	96	24	6
15%	144	36	9	144	36	9
20%	192	48	12	192	48	12
			Number of particles			

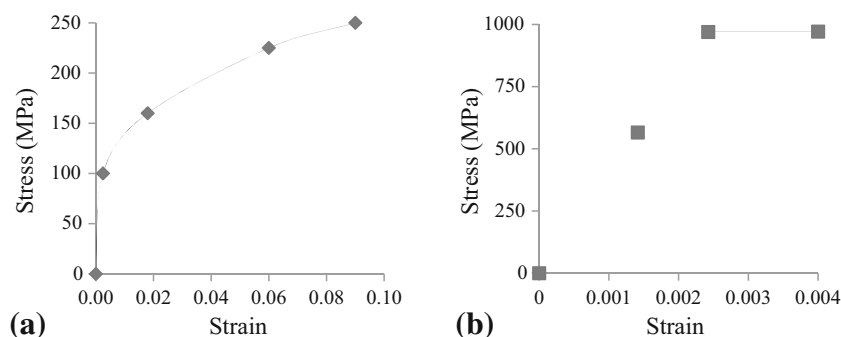| Reinforcement content	Sides of square ☐			Short side of rectangle ▯		
	5.31 µm	10.63 µm	21.27 µm	3.07 µm	6.14 µm	12.28 µm
10%	96	24	6	96	24	6
15%	144	36	9	144	36	9
20%	192	48	12	192	48	12
			Number of particles			

Fig. 2 Stress vs. strain curve for (a) aluminum alloy and (b) silicon carbide particle

3. Results and Analyses

3.1 Stress–Strain Curve

Stress–strain curve is an extremely important graphical presentation of a material's mechanical properties. It is unique for each material and is found by recording the amount of deformation (strain) at distinct intervals of tensile or compressive loading (stress). In this research, firstly, a number of steps were selected from the total number of the computation steps (determined by ANSYS). Then their corresponding displacement values were extracted from the software and the strain values were calculated. To calculate the average stress of the whole block at each of these steps, the partial reaction forces of all nodes at the restrained side of the block were extracted from the software and added together to obtain the total reaction force that was induced by a known displacement (strain) value in that step. These forces were divided by the width of the sample block to calculate the average tensile stresses at various steps, with known strain values. By using these two sets of stress and strain values, the stress–strain curves were plotted for each study case. The displacement was selected +20 µm; therefore, total strain was calculated from Eq 1:

$$\varepsilon = \frac{\Delta l}{l}. \qquad \text{(Eq 1)}$$

where l equaled the length of the sample block.

$$\varepsilon = \frac{20}{329.5} = 0.06.$$

3.1.1 Effect of Reinforcement Content. The effects of the volume percentages of the reinforcement particles, on the stress–strain curves, are shown in Fig. 4 for circular, triangular, square and rectangular particles. All these graphs suggest that the stiffness of the composites was higher than that of matrix materials. The stiffness of MMCs increased with the increase in the reinforcement content. For all types of MMCs considered in this study, the variation in the stiffness was wider when the size of the reinforcement particles was smaller. When the size of the particles was smaller consequently, the total surface between the matrix and particles increased. As the total surface of contact increased, more loads were transferred to the reinforcement particles, and consequently, the total stiffness of the composites increased. This explains the wider variation in stiffness in MMCs with smaller particles. It is also interesting to note that the variation in the stiffness consistently increased when the shape of the reinforcement changed from circle to triangle, to square and to rectangle. However, MMCs with the rectangular particles (Fig. 4g) showed almost similar trend to that of MMCs with the square particles (Fig. 4e). This increase was due to the effect of the shape of the particle on the total surface of contact which was also investigated separately.
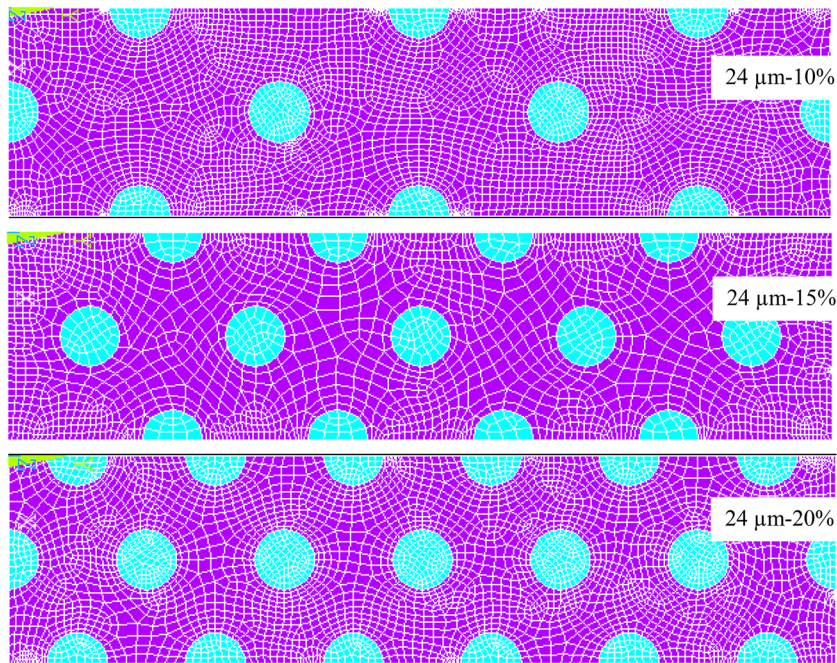
24 µm-10%

24 µm-15%

24 µm-20%

Fig. 3 Meshed case studies—composites with circular particles

3.2 Effect of Size

The effect of the size of the reinforcement particles on the stress–strain curves is shown in Fig. 5 for circular, triangular, square and rectangular particles. These graphs show that effects of the size of the reinforcement particles could not be distinguished when the content of the particles was low (10%). The size effect became prominent when the reinforcement content increased. At higher reinforcement content (20%), the stiffness increased widely with the decrease in the size of the particles. The variation in the stiffness of the MMCs became wider when the shape of the reinforcements changed from circle to triangle to square and to rectangle. However, MMCs with the rectangular particles (Fig. 5h) showed similar trend to that of MMCs with the square particles (Fig. 5f). This increase in the variation was due to the increase in the particle's perimeter and, consequently, increase in the total surface between the matrix and particles. As the total surface of contact increased, more loads were transferred to the reinforcement particles and the total stiffness of the composites increased.

3.2.1 Effect of Shape. To compare the effects of particle's shape on the stress–strain curves, for all four different shapes, all small particle sizes and all large particle sizes were compared separately in two different volume percentages of 10 and 20%. Figures 6 and 7 represent the stress–strain curves for small and large particles, respectively. The figures show that the effects of particle's shape on the stiffness were minor when the reinforcement content was 10%. However, at 20% reinforcement content (Fig. 6b) the effects of particle's shape became clearly visible. As illustrated, the stiffest material was the MMC with rectangular particles followed by square, triangular and circular particles, in order of decreasing stiffness. Similar effects were noted in composites with large particles, as shown in Fig. 7. The reason of this variation in

behavior can be explained by comparing the strain patterns which were produced by these shapes in the composites, as shown in Fig. 8.

As shown in Fig. 8, the pattern of the strain field depended on the particle's shape. Where the strain concentrations occurred, they resulted in a less distributed strain pattern around the particle, in the matrix material. Whatever the strain concentrations were bigger, the less widely and broadly, the strain was distributed throughout the composites. The existence of a high strain concentration increased the possibility of the material failure while a well-distributed strain pattern indicated higher stiffness in the composites. In Fig. 8(a), the maximum strain occurred symmetrically at four points of the circular particle. These points were potentially the debonding points in a fracture, occurring at matrix–particle interface, and as a result of them, the strain pattern in the matrix material showed lower values, compared to the other shapes. In Fig. 8(b), the highest strain concentrations occurred in three places, away from the triangular particle, and the overall strain was better distributed compared to the circular particle. In Fig. 8(c), the highest strain concentrations occurred at two places in matrix, away from the square particle, and also, the distribution of the strain was better than the circular and triangular particles. In Fig. 8(d), the least strain concentrations and the best strain distribution were observed. The MMCs with rectangular particles experienced highest strain hardening over the wide areas of the matrix material; thus, it showed highest stiffness compare to the other shapes of particles. For the same reason, the next high stiffness was seen in the square particle followed by triangular and circular particles.

In addition, the stiffness of the composite can be related to the boundaries around the particles which limit the movements of the dislocations and therefore produce composite with better tensile properties. These boundaries, with minimal elongation
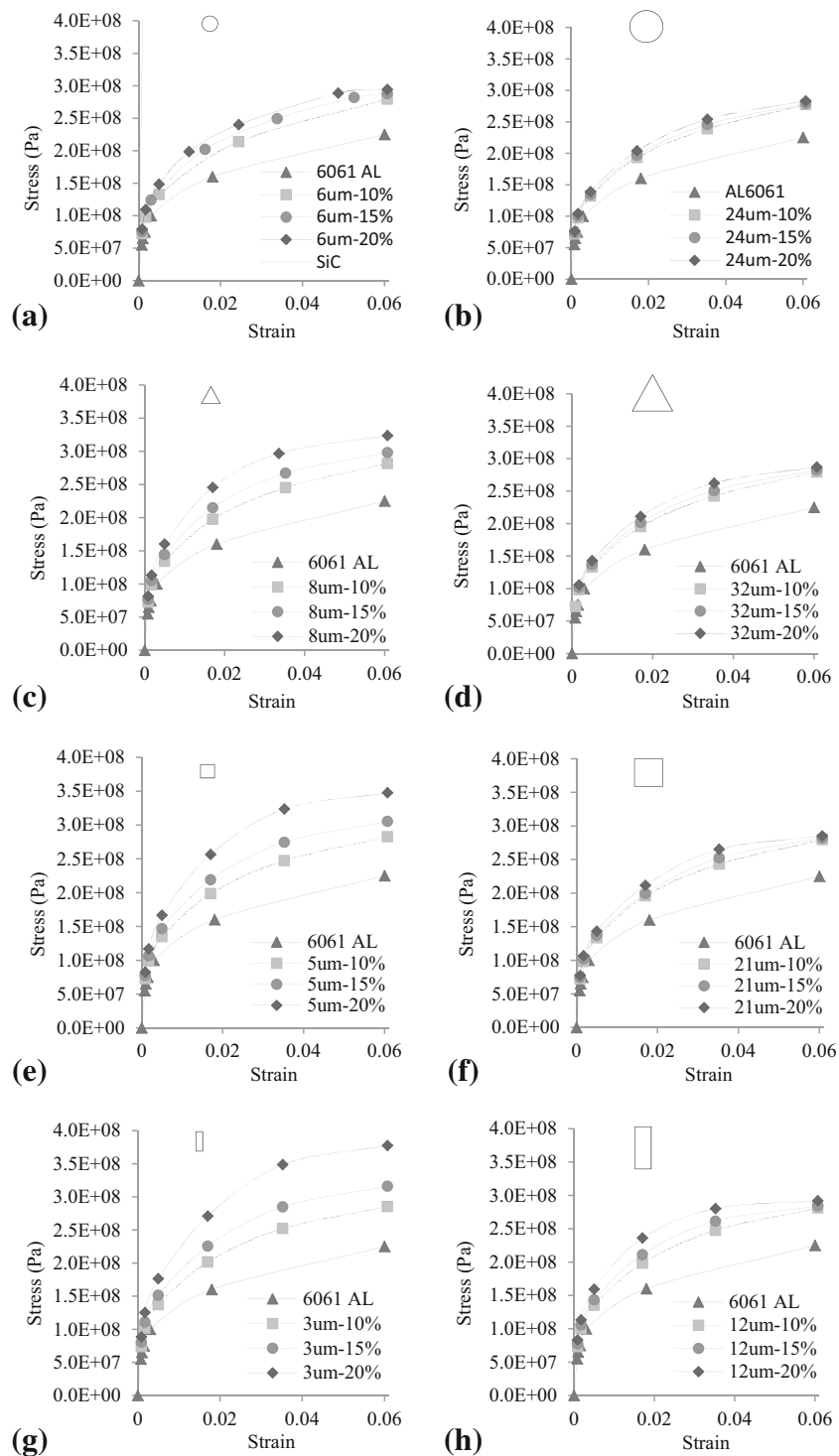
Fig. 4 Stress–strain curves for composites with minimum and maximum particle sizes

(bluish colors), were the maximum for rectangle followed by square, triangle and circle. This also conformed to the stiffness data of these composites.

3.3 Stress Variation

The magnitude and direction of principal stresses, under loading conditions, give indication of possible fracture or particle debonding of MMCs. Therefore, the distribution, direction and magnitude of first and third principal stresses were investigated in and around the particles under the applied displacement.

3.3.1 Effect of Reinforcement Content. To investigate the effect of the reinforcement content on the stress variation, composite with 12-μm-diameter circular particles was selected and its stress vectors' direction and distribution were investigated at the end of the applied displacement, for 10 and 20% reinforcement contents. Figure 9 shows that the third principal stress was much smaller than the first principal stress and the
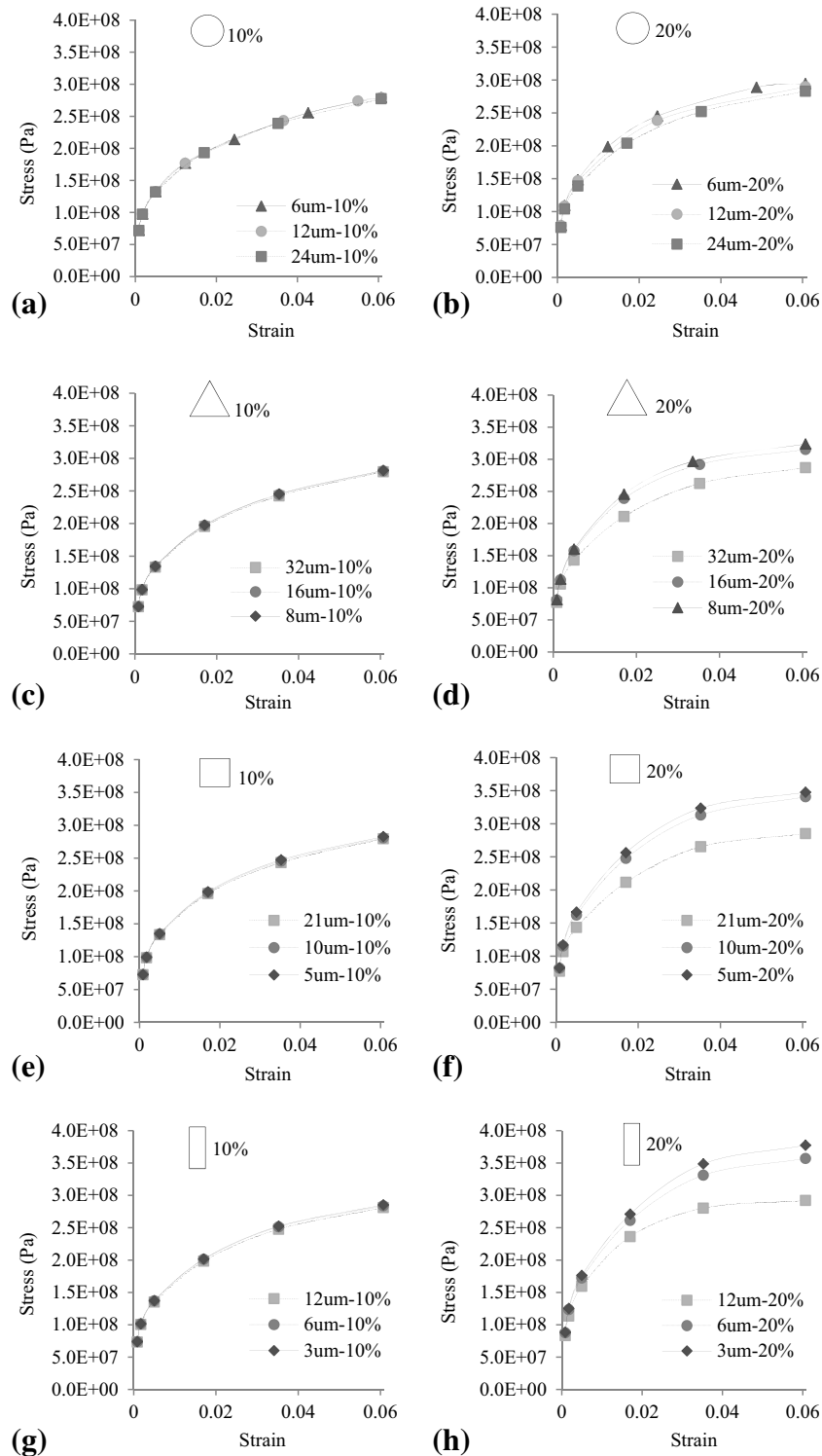
Fig. 5 Stress–strain curves for composites with 10 and 20% reinforcement contents

stresses in the reinforced particles were higher than that of matrix material, irrespective of the reinforcement contents. However, both of the principal stresses increased with the increase in the reinforcement content. This implies as the reinforcement content increased, consequently the stiffness of the composite increased, which resulted in higher stress values.

3.3.2 Effect of Size. Figure 10 shows the effect of particle size on the stress variation, for composites with circular particles and 15% reinforcement content, at the end of the applied displacement. Figure 10 shows that the third principal stress was much smaller than the first principal stress and the stresses in the reinforced particles were higher than that
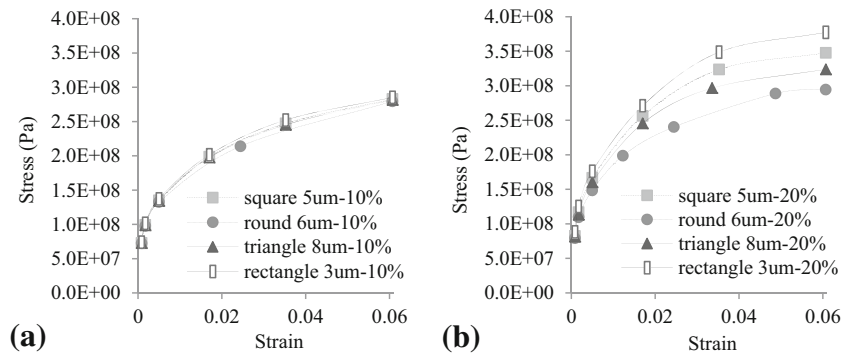
Fig. 6 Stress–strain curves for MMCs with small particles and (a) 10% and (b) 20% contents
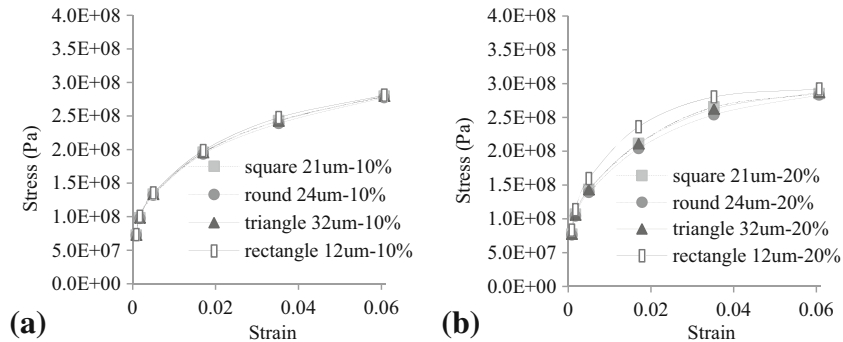

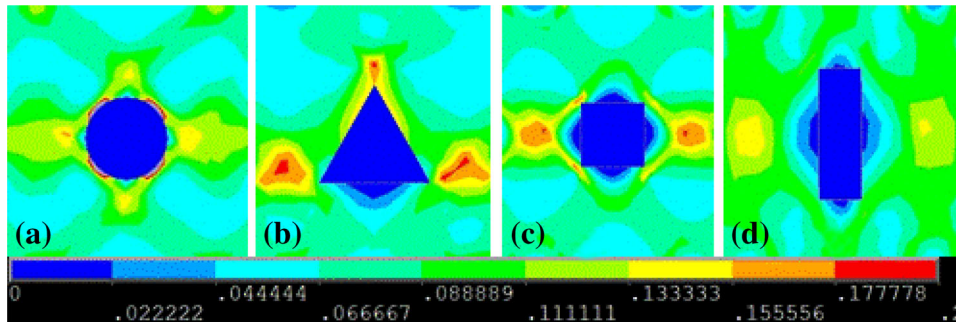**Fig. 7** Stress–strain curves for MMCs with large particles and (a) 10% and (b) 20% contents

Fig. 8 von Mises total strain—15% medium-sized particles content

of matrix material, irrespective of the size of the particles. As shown in the figures, the principal stress magnitudes increased by reducing the particle size.

3.3.3 Effect of Shape. To investigate the effect of particle's shape, composites with medium-sized particles and 15% reinforcement content were selected. The stress vectors' direction and distribution were also shown at three different steps of applied displacement (first, middle and last steps) for all four different particle shapes (Fig. 11, 12, 13, 14).

Figure 11 shows that the directions of stresses did not change from the beginning to the end of the applied displacement for the MMCs, reinforced with circular particles. But when the reinforced particle was triangle, the first principal stresses were in the direction of strain application at the start of the displacement (Fig. 12a). With the increase in the displacement (Fig. 12b), the direction of the stresses changed and the magnitude increased. The direction of the stresses changed mainly around the two sides of the triangular particle as well as

in the matrix just above the particle. The first principal stresses around the sides became parallel to the sides. The stresses in the matrix above the particle rotated away from the sides of the triangle. A similar trend was continued with further increase in the applied displacement (Fig. 12c).

Figure 13 shows the stress distribution in the MMC, reinforced with square particles at different steps of displacement. In this case, no considerable variation in directions of stresses was noted from the beginning to the end of the applied displacement. In the case of rectangular particles (Fig. 14), a trend of divergence of stresses was noted in the matrix, at the top and bottom sides of the particles. The stress distribution was similar to the pattern of magnetic field around a rectangular magnet. This trend was started at the start of the applied displacement and continued until the end of the displacement.

When all the shapes were compared, it was seen that the highest first principal stress was generated in MMC with rectangular particle. In addition, the difference between stresses
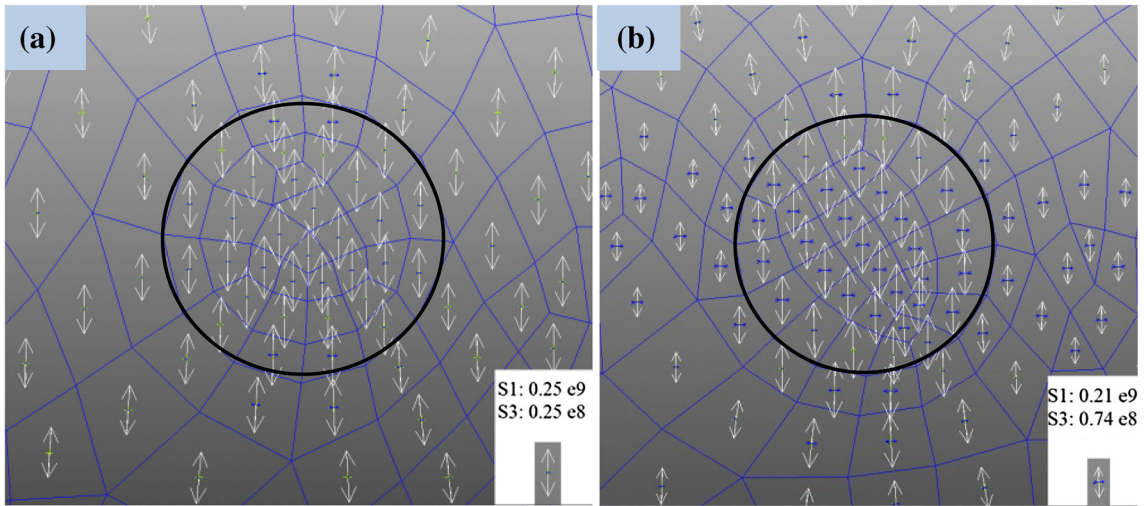
Fig. 9 Stress vector plot for 12 μm (a) 10% and (b) 20% reinforcement content
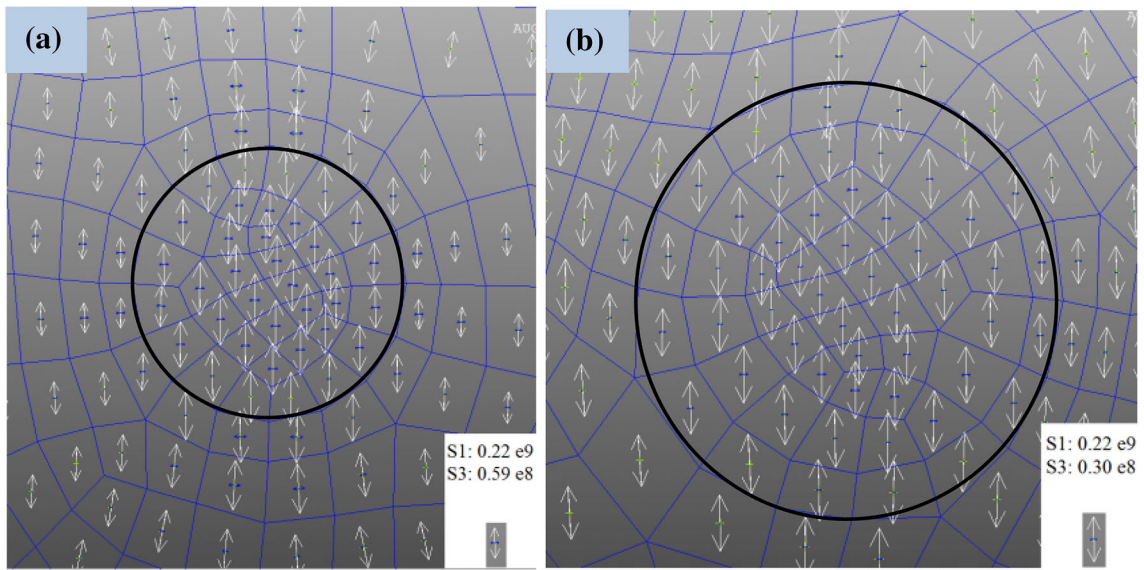

Fig. 10 Stress vector plot for (a) 6 μm-15% and (b) 24 μm-15%

in matrix and reinforcement materials was the maximum for this composite. It is clear from Fig. 11, 12, 13 and 14 that the MMCs with rectangular reinforcements showed highest capability of transferring loads from the matrix material to reinforcement particles, in the loading direction.

However, the triangular particle also carried the loads across the loading direction through the bottom side of the particle and a significant presence of third principal stresses was noted at this side of the particle (Fig. 12). In the case of the square particle, it carried the compressive stresses by the top and bottom side of the particle (Fig. 13). The circular particle also carried the compressive stresses through its middle part, across the loading direction (Fig. 11).

3.4 Development of Plastic Zone

3.4.1 Effect of Reinforcement Content. To investigate the effect of reinforcement content on plasticity, the composites with 12-μm-diameter circular particles were selected; von Mises total strain was plotted for all three different reinforce-

ment contents (Fig. 15). The figure shows that the von Mises stress developed in the matrix partially but symmetrically around the reinforced particles. As the percentage of the reinforcement content increased, the von Mises strain increased and spread across more areas. Very high von Mises strain was noted around the particles when the reinforcement content increased to 20%. This explained the higher stiffness of the MMCs with higher reinforcement contents.

3.4.2 Effect of Size. To investigate the effect of particle size on plasticity, the composites with circular particles and 15% reinforcement content were selected; von Mises total strain was plotted for all sizes (Fig. 16). The figure shows that the von Mises stress developed in the matrix partially but symmetrically around the reinforced particles. With the reduction in particle size, the von Mises strain increased and spread uniformly throughout the matrix material. Almost all the matrix materials were uniformly strained when the particle size reduced to 6-μm-diameter, though little higher strain band was noted in line with the particles, vertical to the applied displacement. The reduction in particles' size increased the
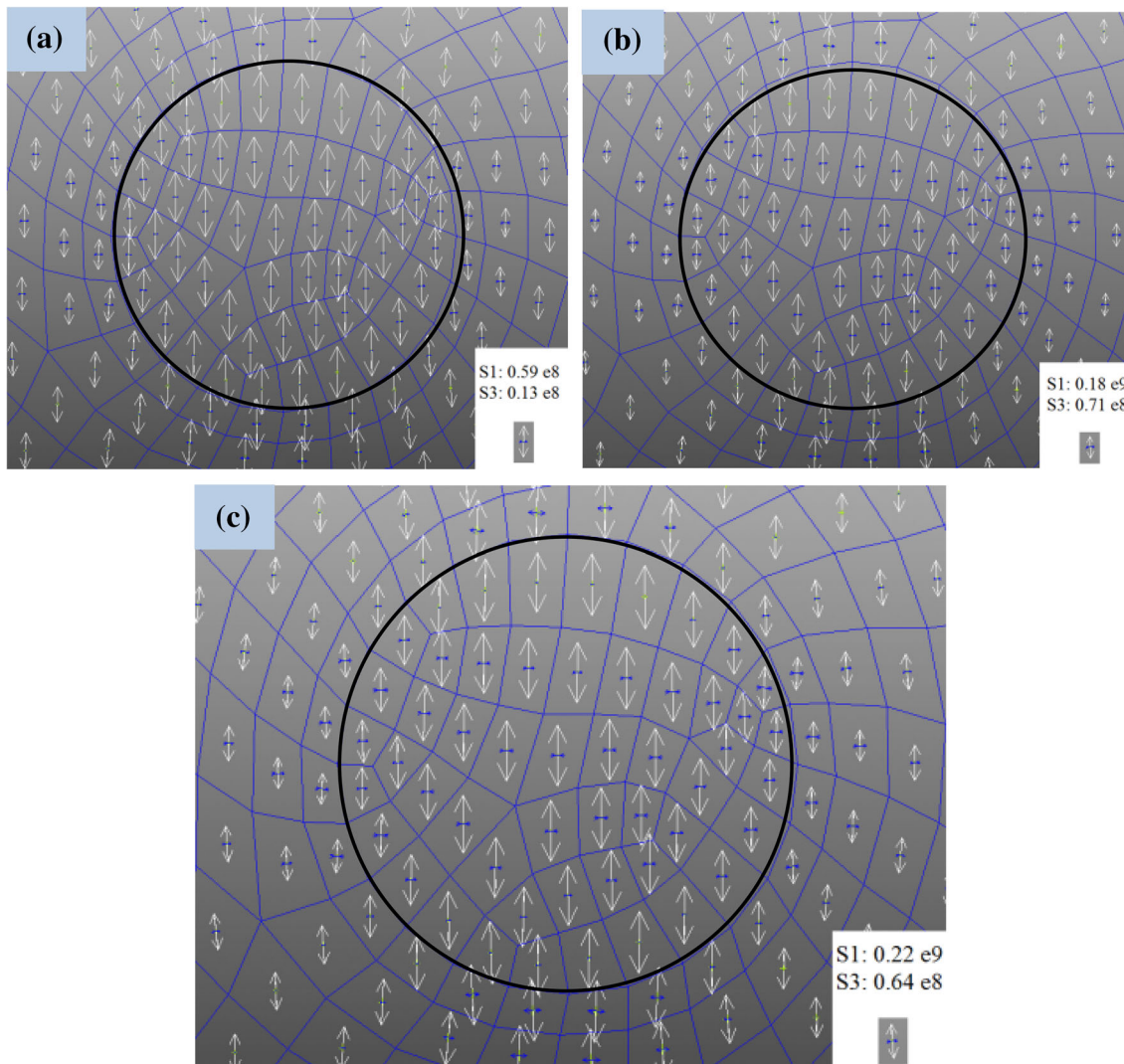
Fig. 11 Stress vector plot for 12 μm-15% circular particle at (a) 0.08% strain, (b) 3.6% strain and (c) 6% strain

particles' total contact surface which consequently increased the total transferred loads to these rigid particles. This explained the better properties of MMCs when the size of the particles was smaller.

3.4.3 Effect of Shape. The effects of particle's shape on plasticity of MMCs, is shown in Fig. 17. It shows that the von Mises stress developed in the matrix partially but symmetrically around the reinforced particles for all of the cases. The spread and amount of strain depended on the shape of the particles. The most widely distributed strain was noted for the MMC with rectangular particles then followed by square to triangular and to circular particles, in order of less strain distribution.

In above figure, two major factors that were involved in the composite behaviors can be observed. The first factor was the effective sides of the particles that limit the movements of the dislocations. As can be seen, circular particles did not have such a factor and the areas around the circular particles were showing large strains; this changed in triangular particles to one effective side that limited the dislocations, and as shown, the minimum strain area was extended around that effective side. Square and rectangular particles each had four effective sides with minimum strain areas all around them. The rectangular particles had more perimeters; therefore, bigger of the minimal

strain areas between the two shapes. This made the composite more rigid by limiting the dislocation movements in tensile condition.

The second factor was the distance between the particles. As the particles were located closer to each other, the matrix material between them became narrower and therefore showed higher strain concentration in that area. This strain concentration was reduced as the shapes changed to rectangle or circle, which provided bigger and better distributed strain areas between the particles. The first factor appeared to be a more conclusive criterion when comparing the composites with different particle shapes.

3.5 Stiffness Comparison

In Table 2, all nine study cases of MMCs with circular particle were arranged based on their stress values for a constant applied strain. It showed that the stiffness of the composites increased with the decrease in the particle size and the increase in the reinforcement content. The stiffness of MMCs depended on the amount of the loads transferred through their hard particles. The transfer of these loads also depended on the amount of the interface between the matrix
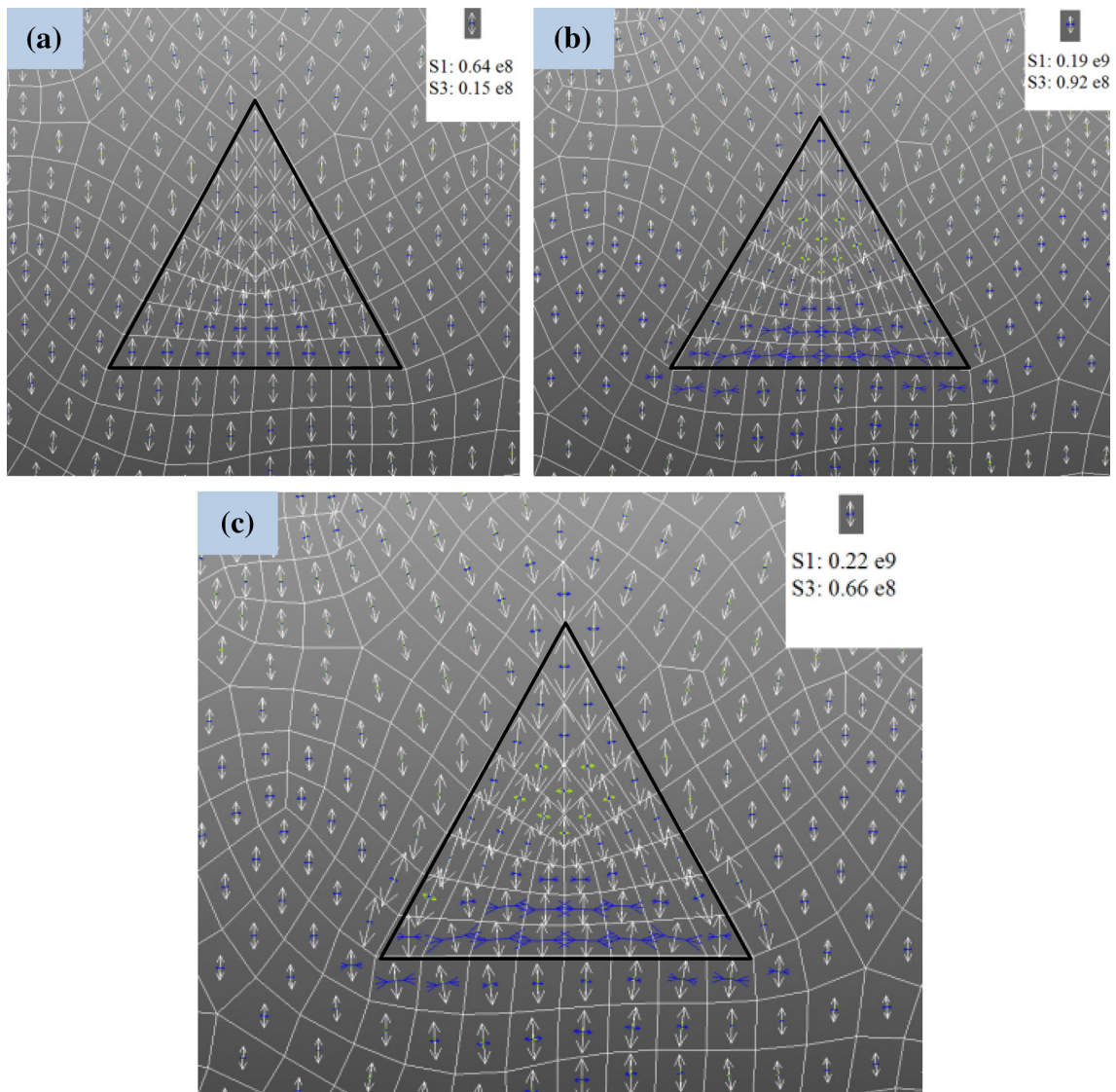
Fig. 12 Stress vector plot for 12 μm-15% triangular particle at (a) 0.08% strain, (b) 3.5% strain and (c) 6% strain

material and hard particles. This interface, or total surface of contact (Sc), was calculated in Eq 2 by using the perimeter of the particles and their content in the composite.

Table 2 shows that the stiffness increased with the increase in the interface length for most of the cases. However, this trend was not always true. For example, the length of interface for MMC with 15% content of 6-μm particles (407.15 μm) was higher than that of MMC with 20% content of 12-μm particles (361.91 μm), but the load-carrying capacity of the latter was higher among these two MMCs. In addition, though MMC with 20% content of 24-μm particles and MMC with 10% content of 6 μm had similar lengths of interface, but the former showed higher stiffness. Therefore, it is clear that the length of matrix–particle interface was not the only factor that contributed to the strengthening mechanism. There are studies that showed that the properties of the matrix materials also contribute to the strengthening mechanism (Ref 8, 14). High reinforcement content (20%) increases the number of particles which apply higher resistance against the deformation of matrix material and induces strain hardening to matrix material. In addition, it also increases the length of interface. On the other hand, when the particle size reduces and

the reinforcement content is constant, the ability for the particles to resist the deformation of matrix material reduces and the particles tend to move with the matrix material (Ref 12, 13). Thus, the matrix material experiences mush less strain hardening with smaller particles compare to that of bigger particles. The strengthening of MMCs occurs mainly by increased length of interface when the reinforcement particles are smaller. Therefore, the content and size of reinforcements contribute to the strengthening mechanism differently. It seems that the combined effects of matrix material hardening and load transfer capability of MMC with 20% content of 12-μm particles made this MMC stronger than that of MMC with 15% content of 6-μm particles. For the similar reasons MMC with 20% content of 24-μm particles was stronger than MMC with 10% content of 6 μm.

$$S_c = \text{Particle perimeter} \times \text{No.of particles} \times \frac{\text{Volumepercentage}}{100}$$

$$\text{(Eq 2)}$$

Similar trend was also noted for MMCs with triangular, square and rectangular particles, as shown in Tables 3, 4 and 5,
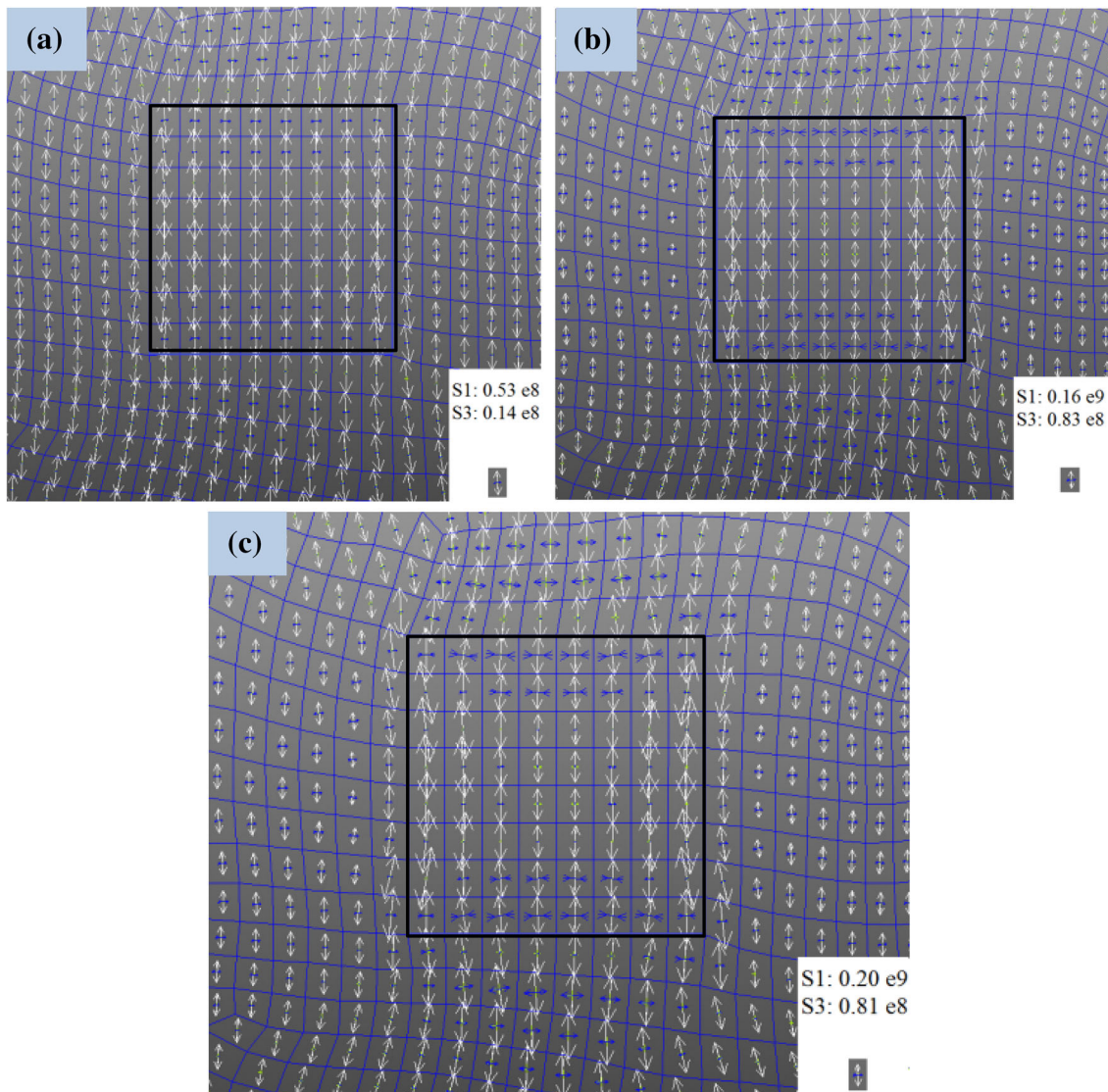
Fig. 13 Stress vector plot for 10 μm-15% square particle at (a) 0.08% strain, (b) 2.9% strain and (c) 6% strain

respectively. Similarly, the combinations of content and size of the particles with strain hardening of the matrix material contributed significantly to the strengthening of the MMCs.

3.6 Compare with Rule of Mixture (ROM)

The rule of mixture is the simplest way to calculate properties of composite materials which only accounts volume or mass percentage of reinforcements. Based on the properties of matrix and reinforced materials, the Young's moduli of the MMCs reinforced with 10, 15 and 20% reinforcements are 104.44, 120.86 and 137.28 GPa, respectively. The simulated results based on 10, 15 and 20% reinforcements of the 12 micron diameter circular shaped particle, the Young's moduli were 93.02, 99.03 and 106.18 GPa, respectively. This shows that the Young's modulus of the MMCs increases with the increase in the content of the reinforcement. This trend is very similar to the primary results obtained in this investigation. In addition, it seems that rule of mixture over estimates the Young's modulus of the MMCs for the considered condition.

4. Discussion

There is no doubt that the presence of reinforcement particles up to a certain amount improved the mechanical properties of MMCs. 20% reinforcement content strengthened MMCs due to the increase in the transferred loads, from the matrix material to the reinforcement particles. This also increased resistance to the flow of matrix material (Ref 7, 12–15). The decrease in particle size increased the interface between the matrix material and reinforcements. This facilitated the transfer of the loads from the matrix material to the reinforcement particles. Particles acted just like obstacles against the movement of matrix during plastic deformation. The yield strength and plastic work hardening rate of the composites increased with decrease in particle size (Ref 4). The composite's strength increased as more tension for the flow of matrix was required (Ref 16). In addition, amount of work hardening was inversely proportional to the particle size and directly proportional to flow stress. Therefore, as the size of the
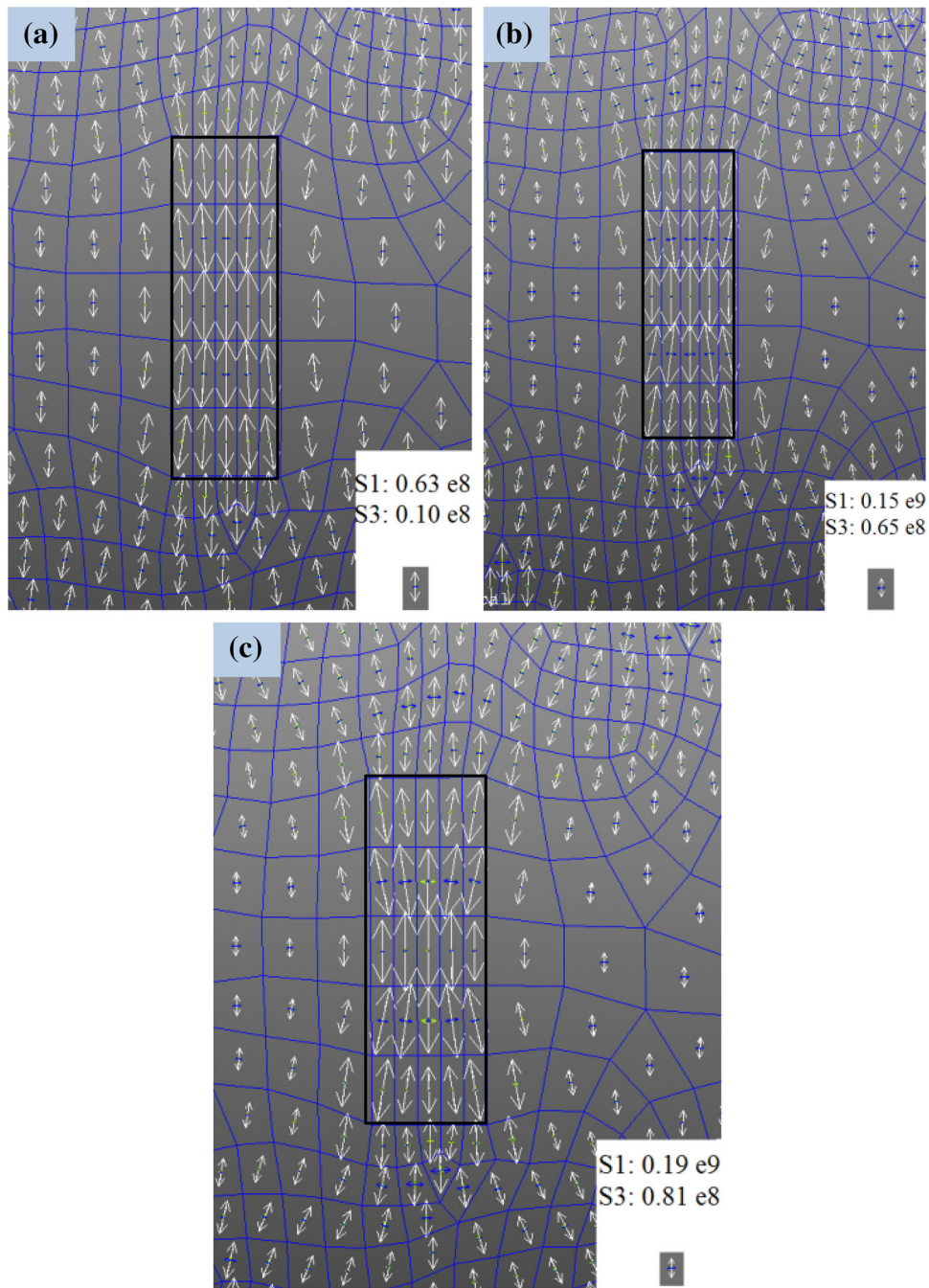
Fig. 14 Stress vector plot for 6 μm-15% rectangular particle at (a) 0.08% strain, (b) 2.3% strain and (c) 6% strain
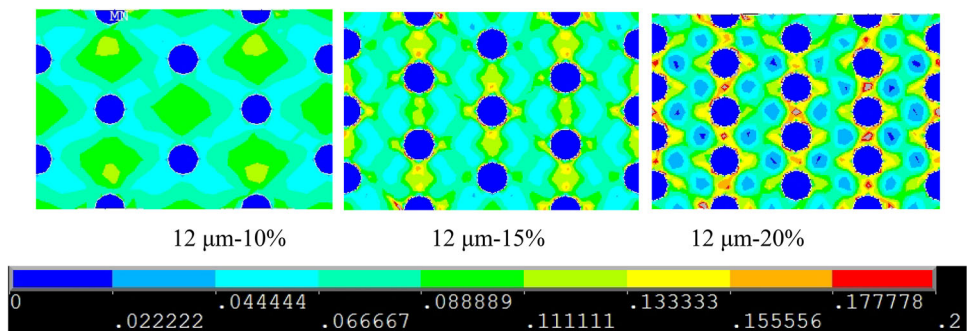

Fig. 15 von Mises total strains in composite with 12-μm-diameter circular particles
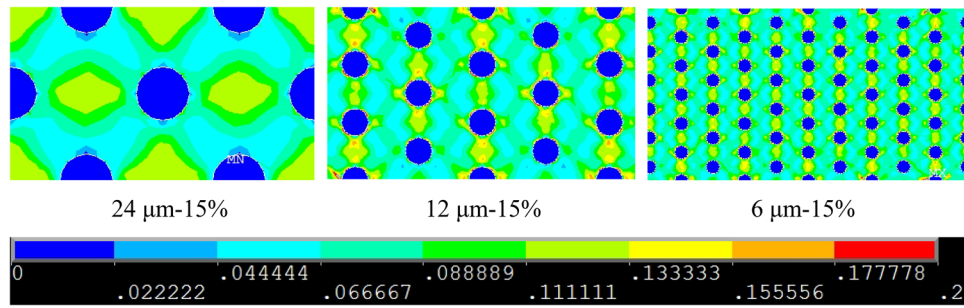
24 μm-15%   12 μm-15%   6 μm-15%

Fig. 16 von Mises total strain plot for composites with 15% circular particles

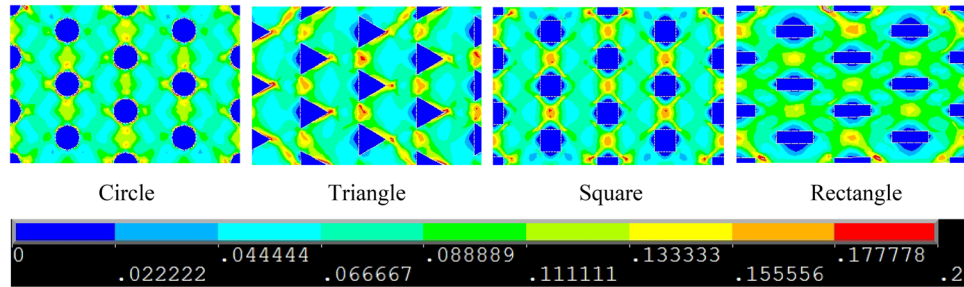Circle   Triangle   Square   Rectangle

Fig. 17 von Mises total strain plot for composites with medium-sized particles-15% volume

Table 2 Stiffness comparison—composites with circular particles

Stress (MPa)	Composite	Max	Absolute increase (%)	Sc (μm)
294	6 μm-20%		30.9	723.82
289	12 μm-20%		28.4	361.91
288	6 μm-15%		28.0	407.15
285	12 μm-15%		26.7	203.58
283	24 μm-20%		25.8	180.96
279	6 μm-10%		24.2	180.96
279	24 μm-15%		24.1	101.79
279	12 μm-10%		24.0	90.48
277	24 μm-10%	Min	23.3	45.24

Table 3 Stiffness comparison—composites with triangular particles

Stress (MPa)	Composite	Max	Absolute increase (%)	Sc
324	8 μm-20%		43.9	930.82
315	16 μm-20%		40.1	465.41
298	8 μm-15%		32.5	523.58
293	16 μm-15%		30.2	261.79
287	32 μm-20%		27.6	232.70
282	32 μm-15%		25.3	130.90
282	8 μm-10%		25.2	232.70
280	16 μm-10%		24.7	116.35
279	32 μm-10%	Min	24.2	58.18

particles decreased, work hardening increased, which in turn led to a higher flow stress (Ref 16). The bigger particles had shorter interface length but displayed more resistance to the movement of matrix material and introduced higher strain hardening in the matrix material. However, the strain hardening played bigger role in strengthening MMCs when the shape of the reinforcements came into the scene in addition to the size and reinforcement content (Ref 9, 17, 18).

The results obtained in this investigation has similarities to the results obtained experimentally by several researchers, such as the mechanical properties, such as tensile strength, of MMCs decreased for a given volume fraction as reinforcement particle size increased (Ref 5-9, 11, 14). Narayanasamy et al. (Ref 11) evaluated the effect of SiC particle size on the workability of Al-SiC composite. It was found that the larger SiC particle (120 μm) gave higher strain hardening index and lower

Table 4 Stiffness comparison—composites with square particles

Stress (MPa)	Composite	Max	Absolute increase (%)	Sc
347	5 μm-20%		54.5	816.69
340	10 μm-20%		51.4	408.35
305	5 μm-15%		35.8	459.39
293	10 μm-15%		30.6	229.69
285	21 μm-20%		26.7	204.18
282	5 μm-10%		25.3	204.17
282	21 μm-15%		25.7	114.85
281	10 μm-10%		24.8	102.09
280	21 μm-10%	Min	24.3	51.05

Table 5 Total surface comparison—composites with rectangular particles

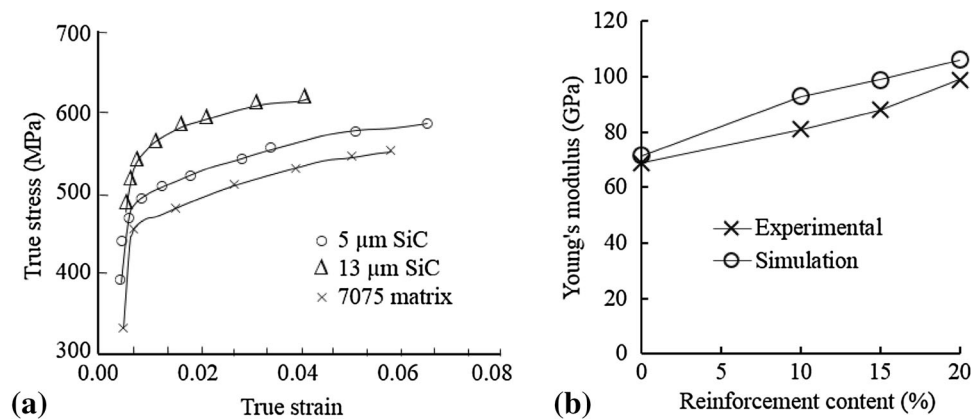| Stress (MPa)	Composite	Max	Absolute increase (%)	Sc
377	3 μm-20%		67.7	943.10
357	6 μm-20%		58.7	471.55
316	3 μm-15%		40.4	530.50
308	6 μm-15%		37.1	265.25
292	12 μm-20%		29.8	235.78
285	3 μm-10%		26.2	235.78
284	12 μm-15%		26.8	132.62
283	6 μm-10%		26.1	117.89
281	12 μm-10%	Min	24.9	58.94

Fig. 18 Comparison of experimental results with simulated results (a) stress–strain curves for different sizes of reinforcements and (b) effect of reinforcement content on Young's modulus for experimental and simulated results

strength coefficient, due to a better load transfer rate of SiC to the aluminum matrix, compared to a smaller particle size. Milan et al. (Ref 14) performed tensile test on T1-Al2124 and Al6061, reinforced with silicon carbide particles (SiC$_P$), and noted that the increase in particle fraction and/or matrix strength increased strength and decreased ductility. On the other hand, an increase in particle size reduced strength and increased the composite ductility. This also noted in this numerical analysis for certain volume percent and shape of the reinforced particles. Tables 2, 3, 4 and 5 present those results. In addition, O'Donnell et al. (Ref 10) and Narayanasamy et al. (Ref 11) noted that the composites with bigger particle had better tensile strength than

those with the smaller particle for 10 and 20% volume contents. Therefore, the MMCs reinforced with the smallest reinforcement particles did not always give the highest strength. Rahimian et al. (Ref 2) experimentally studied properties of aluminum matrix composite considering the particle size and volume fraction of alumina and they found finer particle size of alumina presented greater yield strength of composites. In addition, an increase in the volume percentage, up to 10%, was in favor of the yield strength but above 10% had reverse effect on the strength of the composites.

A direct comparison of the results obtained from above investigation with the experimentally obtained results is not

possible because the experimental arrangement similar to this numerical analysis was never performed. It addition, (1) it is not easy to manufacture MMCs reinforced with particles of a particular shape and (2) arranging MMCs with the configurations discussed in the investigation is very expensive and difficult. However, a qualitative comparison with experimental studies can be presented.

Experimental investigations performed by many researchers (Ref 7, 19-21) reported that stiffness of MMCs increases with the increase in the volume fraction of the reinforced particles. Jamaati et al. (Ref 20) experimentally found that when the proper bonding and distribution of reinforced particles are achieved, the tensile strength of the composite strip with larger particle size became less than the composite with smaller particle size (Ref 7, 21).

In Fig. 18(a), experimentally obtained stress–strain curves for different particle sizes have been presented based on the Ref 22. It shows that the shape of stress strain curves is very similar to what obtained in this study. It also shows that bigger particle sizes gives higher stiffness to the MMCs. Figure 18(b) compares experimentally (Ref 23) obtained Young's modulus with that obtain from the simulation in this study when the content of reinforcement varies. It shows that the Young's modulus increases with the increase in reinforcement content, and the experimental and simulated results increase in parallel with the increase in reinforcement content. In this case, simulated results slightly over estimate Young's modulus which may be due to irregular shape and non-uniform distribution of reinforcements for the experimental case.

5. Conclusion

Based on the FEA analyses of MMCs with four different shapes of particles, each with three different sizes and three different volume percentages, total thirty-six study cases were investigated under a constant positive displacement and the following conclusions were drawn:

1. The effects of shape and size of the reinforcement particles on the tensile properties of MMCs were negligible when the reinforcement content was 10%.
2. The MMCs with rectangular particles showed highest stiffness, compared to the other MMCs under similar conditions. Also, strain pattern was most widely and evenly distributed in the matrix material and around the rectangular particles.
3. The first principal stresses acted along the direction of the applied displacement and their direction remained unchanged for all of the cases, except for the MMCs with triangular particles. In these cases, the stresses around the interface tended to align with the two sides of the triangular particles. Reasonably bigger third principal stresses were noted around the bottom interface of the triangle. The rectangular particles experienced the highest first principal stresses among all other shapes considered in this study. Thus, the MMCs with rectangular particles showed the highest stiffness.
4. The stiffness of MMCs depended not only on the length of the interface, which facilitated the transfer of the loads from matrix material to particles, but also on the state of

the matrix material which was influenced by the shape, size and reinforcement content.
5. There was an optimum combination of shape, size and reinforcement content for which the highest stiffness of MMCs could be achieved.

References

1. H. Huang and M. Bush, Finite element analysis of mechanical properties in discontinuously reinforced metal matrix composites with ultrafine micro structure, *Mater. Sci. Eng. A*, 1997, **232**(1), p 63–72
2. M. Rahimian, N. Parvin, and N. Ehsani, Investigation of particle size and amount of alumina on microstructure and mechanical properties of Al matrix composite made by powder metallurgy, *Mater. Sci. Eng. A*, 2010, **527**(4), p 1031–1038
3. S.B. Prabu, L. Karunamoorthy, and G. Kandasami, A finite element analysis study of micromechanical interfacial characteristics of metal matrix composites, *J. Mater. Process. Technol.*, 2004, **153**, p 992–997
4. Y. Yan, L. Geng, and A. Li, Experimental and numerical studies of the effect of particle size on the deformation behavior of the metal matrix composites, *Mater. Sci. Eng. A*, 2007, **448**(1), p 315–325
5. V.K. Varma, S.V. Kamat, Y.R. Mahajan, and V.V. Kutumbarao, Effect of reinforcement size on low strain yielding behaviour in Al-Cu-Mg/SiCp composites, *Mater. Sci. Eng. A*, 2001, **318**(1–2), p 57–64
6. Z. Wang, M. Song, C. Sun, and Y. He, Effects of particle size and distribution on the mechanical properties of SiC reinforced Al-Cu alloy composites, *Mater. Sci. Eng. A*, 2011, **528**(3), p 1131–1137
7. N. Chawla, C. Andres, J.W. Jones, and J.E. Allison, Effect of SiC volume fraction and particle size on the fatigue resistance of a 2080 Al/SiCp composite, *Metall. Mater. Trans. A*, 1998, **29**(11), p 2843–2854
8. J.N. Hall, J. Wayne Jones, and A.K. Sachdev, Particle size, volume fraction and matrix strength effects on fatigue behavior and particle fracture in 2124 aluminum-SiCp composites, *Mater. Sci. Eng. A*, 1994, **183**(1–2), p 69–80
9. V.V. Ganesh and N. Chawla, Effect of reinforcement-particle-orientation anisotropy on the tensile and fatigue behavior of metal-matrix composites, *Metall. Mater. Trans. A Phys. Metall Mater. Sci.*, 2004, **35**(1), p 53–61
10. G. O'Donnell and L. Looney, Production of aluminium matrix composite components using conventional PM technology, *Mater. Sci. Eng. A*, 2001, **303**(1–2), p 292–301
11. R. Narayanasamy, T. Ramesh, and M. Prabhakar, Effect of particle size of SiC in aluminium matrix on workability and strain hardening behaviour of P/M composite, *Mater. Sci. Eng. A*, 2009, **504**(1–2), p 13–23
12. A. Pramanik, L. Zhang, and J. Arsecularatne, An FEM investigation into the behavior of metal matrix composites: tool–particle interaction during orthogonal cutting, *Int. J. Mach. Tools Manuf.*, 2007, **47**(10), p 1497–1506
13. A. Pramanik, L. Zhang, and J. Arsecularatne, Micro-indentation of metal matrix composites—an FEM analysis, *Key Eng. Mater.*, 2007, **340**, p 341
14. M.T. Milan and P. Bowen, Tensile and fracture toughness properties of SiCp reinforced Al alloys: effects of particle size, particle volume fraction, and matrix strength, *J. Mater. Eng. Perform.*, 2004, **13**(6), p 775–783
15. A. Pramanik, L. Zhang, and J. Arsecularatne, Deformation mechanisms of MMCs under indentation, *Compos. Sci. Technol.*, 2008, **68**(6), p 1304–1312
16. A.M. Al-Qutub, I.M. Allam, and T.W. Qureshi, Effect of sub-micron Al2O3 concentration on dry wear properties of 6061 aluminum based composite, *J. Mater. Process. Technol.*, 2006, **172**(3), p 327–331
17. N. Chawla and Y.L. Shen, Mechanical behavior of particle reinforced metal matrix composites, *Adv. Eng. Mater.*, 2001, **3**(6), p 357–370
18. C. Sun, M. Song, Z. Wang, and Y. He, Effect of particle size on the microstructures and mechanical properties of SiC-reinforced pure aluminum composites, *J. Mater. Eng. Perform.*, 2011, **20**(9), p 1606–1612
19. C.-Y. Chen and C.-G. Chao, Effect of particle-size distribution on the properties of high-volume-fraction SiC p-Al-based composites, *Metall. Mater. Trans. A*, 2000, **31**(9), p 2351–2359

20. R. Jamaati, S. Amirkhanlou, M.R. Toroghinejad, and B. Niroumand, Effect of particle size on microstructure and mechanical properties of composites produced by ARB process, *Mater. Sci. Eng. A*, 2011, **528**(4), p 2143–2148

21. M. Kok, Production and mechanical properties of Al_2O_3 particle-reinforced 2024 aluminium alloy composites, *J. Mater. Process. Technol.*, 2005, **161**(3), p 381–387

22. T.J.A. Doel and P. Bowen, Tensile properties of particulate-reinforced metal matrix composites, *Compos. A Appl. Sci. Manuf.*, 1996, **27**(8), p 655–665

23. I.A. Ibrahim, F.A. Mohamed, and E.J. Lavernia, Particulate reinforced metal matrix composites—a review, *J. Mater. Sci.*, 1991, **26**(5), p 1137–1156